

## Growth of Tabular $\alpha$ -Al<sub>2</sub>O<sub>3</sub> Grains on Porous Alumina Substrate

Bang-Ying Yu and Wen-Cheng J. Wei<sup>†</sup>

Department of Materials Science and Engineering, National Taiwan University, Taiwan 106, Republic of China

**Gradient, porous alumina ceramics were prepared with the characteristics of microsized tabular  $\alpha$ -Al<sub>2</sub>O<sub>3</sub> grains grown on a surface with a fine interlocking feature. The samples were formed by spin-coating diphasic aluminosilicate sol on porous alumina substrates. The sol consisted of nano-sized pseudo-boehmite (AlOOH) and hydrolyzed tetraethyl orthosilicate [Si(OC<sub>2</sub>H<sub>5</sub>)<sub>4</sub>]. After drying and sintering at 1150°–1450°C, the crystallographic and chemical properties of the porous structures were investigated by analytical electron microscopy. The results show that the formation of tabular  $\alpha$ -Al<sub>2</sub>O<sub>3</sub> grains is controlled by the dissolution of fine Al<sub>2</sub>O<sub>3</sub> in the diphasic material at the interface. The nucleation and growth of tabular  $\alpha$ -Al<sub>2</sub>O<sub>3</sub> grains proceeds heterogeneously at the Al<sub>2</sub>O<sub>3</sub>/glass interface by ripening nano-sized Al<sub>2</sub>O<sub>3</sub> particles.**

### I. Introduction

ANISOTROPIC grains with interlocking or texture structure are interesting because greater constraints among grains could enhance the bonding stress of ceramic matrixes. Al<sub>2</sub>O<sub>3</sub> is one of the well-known structural ceramics with acceptable mechanical and chemical properties.<sup>1</sup> Tabular (or plate-like) alumina grains could be formed by an aluminosilicate gel method,<sup>2</sup> hot pressing and sinter forging processing,<sup>3</sup> or oxidation of Al metal with alumina powder.<sup>4</sup> Seabaugh and colleagues<sup>5–7</sup> have reported that anisotropic Al<sub>2</sub>O<sub>3</sub> grains were formed by the addition of various oxides, for instance, SiO<sub>2</sub>, CaO, and TiO<sub>2</sub>. When the mixture was sintered above the eutectic temperature of the system (Al<sub>2</sub>O<sub>3</sub>–MO), a liquid phase was formed to help fast diffusion. Besides, a reduction of the surface energy of  $\alpha$ -Al<sub>2</sub>O<sub>3</sub> resulted in the fast grain growth of Al<sub>2</sub>O<sub>3</sub> along specific crystalline planes. Without the doped material, there was no anisotropic growth of Al<sub>2</sub>O<sub>3</sub> grains.<sup>8</sup> The key point of abnormal alumina grain growth is the presence of a multiple-component-oxide liquid phase during sintering.

Previous literature<sup>9</sup> has demonstrated mullite synthesis from diphasic aluminosilicate gels with stoichiometric and nonstoichiometric compositions. The pseudo-boehmite would convert to  $\gamma$ - and  $\delta$ -Al<sub>2</sub>O<sub>3</sub>, at temperatures around 400° and 1050°C, respectively, and then react with amorphous SiO<sub>2</sub> to form mullite in stoichiometric diphasic gel at 1200°C. Mullite grains grew from the diphasic matrix with an equal-axis shape. Our previous study<sup>10</sup> found that tabular grains formed on porous Al<sub>2</sub>O<sub>3</sub> substrate below the eutectic temperature,  $T_e = 1570^\circ\text{C}$ . However, several important issues were not clarified, i.e., the formation mechanism and the crystalline phase of the tabular grains. This study identified the crystalline phase and

investigated the formation mechanism of tabular  $\alpha$ -Al<sub>2</sub>O<sub>3</sub> grains. Microstructural observation revealed the formation of a glassy phase at processing temperatures below the eutectic point ( $T_e$ ) and we reported the composition of the glass.

### II. Experimental Procedure

The morphology and particle size of pseudo-boehmite (Remel-A-20, Remet, Utica, NY) by transmission electron microscopy (TEM) show a platy shape with a narrow size distribution. The size range was from 5 to 30 nm, and no particles were bigger than 50 nm. Porous Al<sub>2</sub>O<sub>3</sub> substrate was made by slip casting a slurry containing alumina powder (A16-SG, Alcoa Co., Pittsburgh, PA) and dispersant (Darven-C, ammonium salt of polymethylacrylic acid, R. T. Vanderbilt Co., Norwalk, CT). The tape normally has a thickness of 0.5 mm and the processing details were reported in a previous study.<sup>11</sup> After heat treatment at 1100°C for 1 h, the sample had a granular microstructure (Fig. 1(a)) with a density of 63%  $\pm$  1% theoretical density, and designated as G11. The G11 tape was slightly sintered and the mean size of the Al<sub>2</sub>O<sub>3</sub> grains was 0.5  $\mu\text{m}$ .

Three coating sols were prepared by the same sol–gel process. Diphasic 60AS sol is composed of SiO<sub>2</sub>/Al<sub>2</sub>O<sub>3</sub> in a 2/3 molar ratio. Tetraethyl orthosilicate (TEOS, Art. 800658, Merck-Schuchardt, Hohenbrunn, Germany), pseudo-boehmite, ethanol (purity 99.5%, Nihon Shiyaku Industry Ltd., Osaka, Japan), and deionized water were used to prepare the 60AS sol. TEOS was dissolved in ethanol and hydrolyzed by H<sub>2</sub>O in acidic condition (pH = 2.0) by HCl solution. After mixing for 30 min, the pseudo-boehmite colloids were added and stirred for 1 h. The formulation of the precursor mixture in molar ratio is SiO<sub>2</sub>:Al<sub>2</sub>O<sub>3</sub>:H<sub>2</sub>O:ethanol = 1.0:1.5:28.0:2.7. Experimental details have been described previously.<sup>12</sup> Pure SiO<sub>2</sub> sol and pseudo-boehmite sol were also prepared as the comparison cases, which were prepared either from acidic TEOS solution or the pseudo-boehmite precursor, respectively.

These sols were spin coated at a rate of 1000–5000 rpm for 10 s on porous Al<sub>2</sub>O<sub>3</sub> substrates as the viscosity of the diphasic sol reached 35 cP. The Al<sub>2</sub>O<sub>3</sub> substrates were named G11S, G11A, and G11M after being coated by a sol of silica, alumina, and 60AS, respectively. G11A and G11M showed coating layers about half to several micrometers in thickness. The coating layer on G11S can hardly be detected due to the filling of the low-viscous SiO<sub>2</sub> sol (ca. 35 cP) into the porous Al<sub>2</sub>O<sub>3</sub> substrate. After coating, the samples were dried at 25°C for a day. Then the samples were heated at a rate of 10°C/min to 1150°–1450°C for 1 h. The sintering was conducted in a high-purity Al<sub>2</sub>O<sub>3</sub> tube and no contaminants from low-melting salts, e.g., NaCl, were present.

The morphologies of the samples were observed by field emission scanning electron microscopy (Instrument 1530, Leo, Cambridge, U.K.) equipped with energy-dispersive spectrometry (EDS, DX4, EDAX Corp., Mahwah, NJ). Detailed microstructures and crystalline phase were also analyzed by analytical electron microscopy (AEM, TEM 100CX, JEOL Co., Akishima, Japan, and TECNAI F30 and TECNAI 20, Philips Co., Almelo, the Netherlands) and X-ray diffractometry (XRD, Philips PW1710, Eindhoven, the Netherlands).

A. Pyzik—contributing editor

Manuscript No. 23280. Received May 30, 2007; approved October 1, 2007.  
Part of funding from National Cheng-Kung University and National Science Council (NSC87-2622-E-002-014) in Taiwan is greatly appreciated.

<sup>†</sup>Author to whom correspondence should be addressed. e-mail: wjwei@ntu.edu.tw

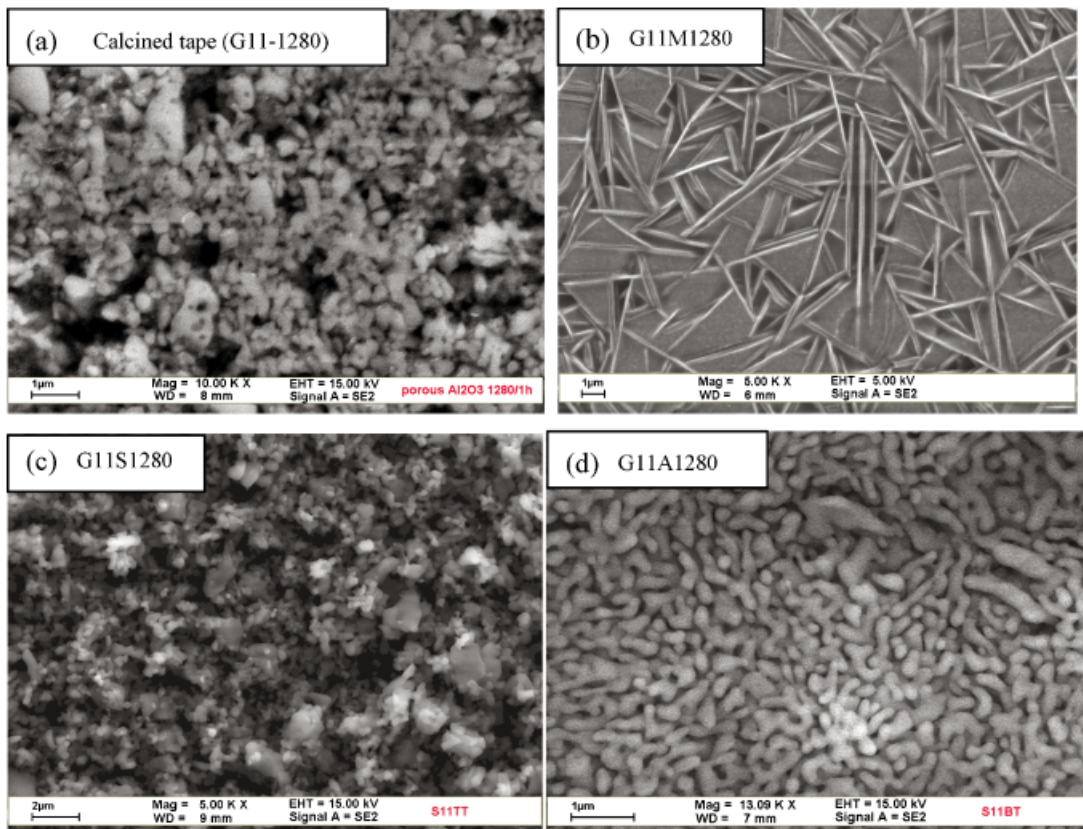


Fig. 1. Scanning electron microscopy micrographs showing (a) calcined porous  $\text{Al}_2\text{O}_3$  substrate, G111280, (b) G11M1280, (c) G11S1280, and (d) G11A1280. The samples were precalcined at  $1100^\circ\text{C}$  before coating and then sintered at  $1280^\circ\text{C}$  for 1 h after coating.

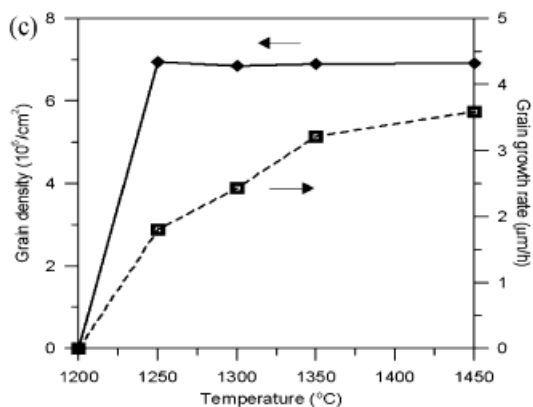
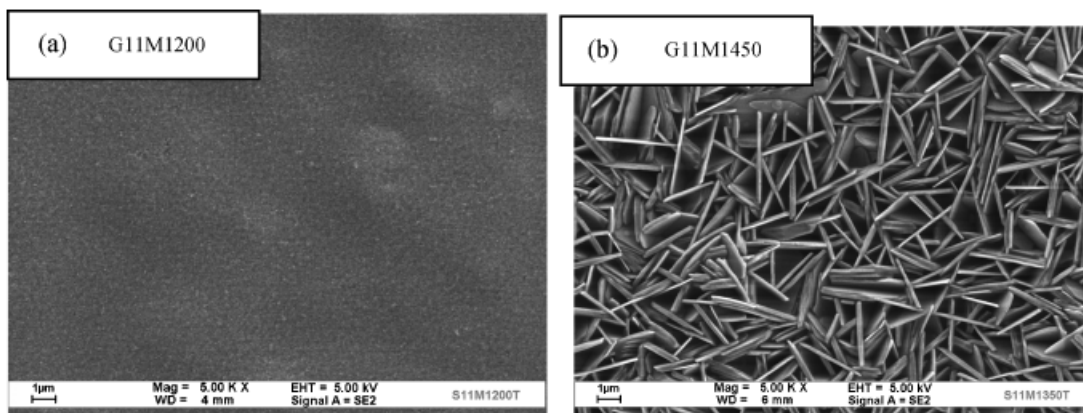


Fig. 2. Scanning electron microscopy of the surface morphology of (a) G11M1200, (b) G11M1450, and (c) the grain density and grain growth rate plotted against sintering temperature.

### III. Results and Discussion

Figure 1(b) shows the top view of G11M1280, illustrating tabular  $\alpha$ -Al<sub>2</sub>O<sub>3</sub> grains in the coating film grown in a direction perpendicular to the surface and interlaced. The tabular grains were up to 8  $\mu$ m in length, about 0.2- $\mu$ m thick, with aspect ratios from 3 to 20.

The other two samples, G11S1280 and G11A1280, are shown in Figs. 1(c) and (d), respectively. G11S1280 with SiO<sub>2</sub> sol coating showed no apparent coating. On the G11A1280 sample, a vermicular structure was seen on the surface of the coating.

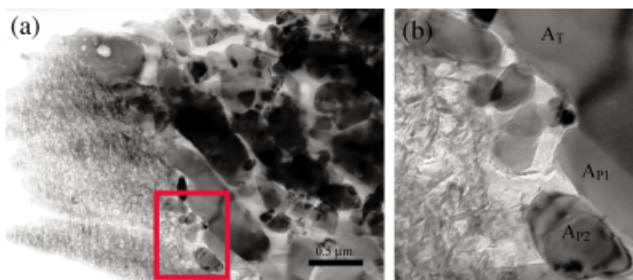
The crystal structures of the coatings were analyzed by XRD. The coating samples had only  $\alpha$ -Al<sub>2</sub>O<sub>3</sub> except for sample G11M1280, which showed an additional very small peak at 20.3°, possibly belonging to cristobalite (SiO<sub>2</sub>).

Figure 2 shows the surface morphologies of G11M sintered at 1200°–1450°C for 1 h. No tabular grains were observed on the sample sintered at 1200°C. As the sintering temperature increased to 1350°C, the glassy surface was replaced with porous structure consisting of tabular  $\alpha$ -Al<sub>2</sub>O<sub>3</sub> grains with an interlocking configuration.

The grain density of tabular  $\alpha$ -Al<sub>2</sub>O<sub>3</sub> grains on the surface of the G11M sample sintered at different temperatures is shown in Fig. 2(c). Below 1250°C, the grain density was zero because there were no tabular  $\alpha$ -Al<sub>2</sub>O<sub>3</sub> grains on the surface. The grain density on the surface of the G11M above 1250°C is almost the same,  $7 \times 10^6$  cm<sup>-2</sup>. This means that instant heterogeneous nucleation of tabular  $\alpha$ -Al<sub>2</sub>O<sub>3</sub> grains occurred at  $\geq 1250^\circ$ C. Nucleus formation takes place seemingly independent of the temperature at  $\geq 1250^\circ$ C. However, we believe some nuclei have formed at as low as 1150°C (as shown in Fig. 3(b)). The grain growth rate of tabular  $\alpha$ -Al<sub>2</sub>O<sub>3</sub> grains on the surface increased from 1.8 to 3.6  $\mu$ m/h when the sintering temperature was raised from 1250° to 1450°C.

Nucleus formation and growth of tabular  $\alpha$ -alumina is controlled by the solubility of alumina in glass, which is dependent on temperature. Nucleus formation of tabular  $\alpha$ -alumina takes place at the interface of glass/ $\alpha$ -alumina. Further growth of the nucleus is hindered due to insufficient space existing around the grains. That is why we observed nearly identical grain density on the surface of G11M above 1250°C.

Figure 3 shows the cross-sectional TEM morphologies of G11M1150, illustrating a typical structure of a few tabular  $\alpha$ -Al<sub>2</sub>O<sub>3</sub> grains grown at the interface of glass/ $\alpha$ -Al<sub>2</sub>O<sub>3</sub> grain. Porous substrate, tabular  $\alpha$ -Al<sub>2</sub>O<sub>3</sub> grains (A<sub>T</sub>), and acicular nano-grains could be observed at the interface. The tabular grains were in the middle of growth, but not large enough to reach the surface of the coating layer. Hence the morphology of the top view on the G11M1150 sample was covered by diphasic materials, similar to that of G11M1200 (Fig. 2(a)). There are some small grains (A<sub>P</sub>) that have nontabular characters, which develop faceted low-index surfaces. The grain coalescence of the A<sub>P1</sub> grain with its neighboring A<sub>T</sub> grain could result in large tabular grains as those in the middle region of Fig. 3(a). Grain coalescence was also occasionally found in the G11M1280



**Fig. 3.** Cross-sectional transmission electron microscopy morphologies of G11M1150. (a) The interface of diphasic (left) and porous Al<sub>2</sub>O<sub>3</sub> (right) regions and (b) the region of interest, showing pretabular grains (A<sub>P</sub>) next to tabular grains (A<sub>T</sub>), nano-acicular grains, and glassy phase.

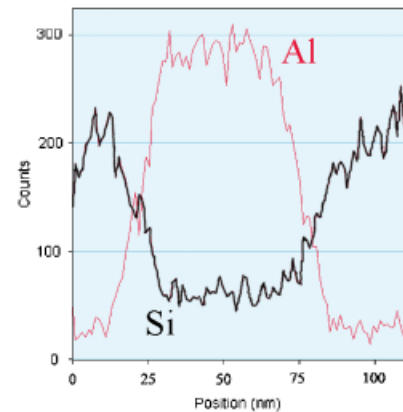
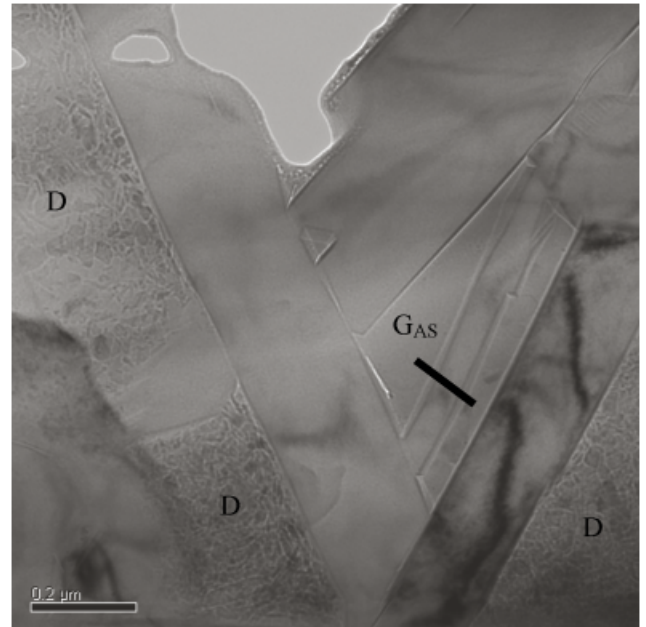


**Fig. 4.** Transmission electron microscopy micrograph of G11M1250 illustrating the elemental scanning results of Al and Si contents. The D regions are diphasic, containing fine Al<sub>2</sub>O<sub>3</sub> grains.

samples. A few tabular  $\alpha$ -Al<sub>2</sub>O<sub>3</sub> grains that contained small angle boundaries and dislocations have been characterized previously.<sup>13</sup> These observations reveal the rearrangement of small Al<sub>2</sub>O<sub>3</sub> grains to the lowest surface energy and then the formation of tabular  $\alpha$ -Al<sub>2</sub>O<sub>3</sub> grains.

The composition of an amorphous region near tabular  $\alpha$ -Al<sub>2</sub>O<sub>3</sub> grains (Fig. 4) was analyzed by analytical TEM. The composition of the tabular  $\alpha$ -Al<sub>2</sub>O<sub>3</sub> grains in the coating layer was confirmed. Moreover, there were two types of grain boundary phases. One (marked D in Fig. 4(a)) was a diphasic region with cuboid nano-sized Al<sub>2</sub>O<sub>3</sub> grains. These could be  $\delta$ - or  $\theta$ -Al<sub>2</sub>O<sub>3</sub>,<sup>14</sup> with a SiO<sub>2</sub>/Al<sub>2</sub>O<sub>3</sub> molar ratio of about 17/83. This is higher in Al<sub>2</sub>O<sub>3</sub> content than in mullite, 40/60. No other elements, e.g., Na<sub>2</sub>O or MgO, were detected. The other type of grain boundary phase was glass marked as G<sub>AS</sub> in Fig. 4. The composition of the glassy phase was about 4.7-mol% Al<sub>2</sub>O<sub>3</sub> and 95.3-mol% SiO<sub>2</sub>. EDS results from a number of glassy regions showed an Al<sub>2</sub>O<sub>3</sub> content of  $5 \pm 2$  mol%. As the temperature increases, more Al dissolves in the glass. This may play a role in enhancing diffusion during the growth of tabular grains.

The AEM result of electron diffraction analyses (not shown here) in Fig. 4 indicates that there are no crystalline phases in the glassy region G<sub>AS</sub>. Minor Al<sub>2</sub>O<sub>3</sub> (by EDS) was detected, which implies Al–O dissolution into amorphous SiO<sub>2</sub>. This provides decisive evidence that transient glassy phases exist in the Al<sub>2</sub>O<sub>3</sub>–SiO<sub>2</sub> system below the eutectic temperature.

#### IV. Conclusions

In summary, analysis of nano- $\text{Al}_2\text{O}_3$  particles transformed from pseudo-boehmite resulted in the following conclusions. First, alumina dissolves into a glassy  $\text{SiO}_2$  phase and acts as the source of growing tabular  $\text{Al}_2\text{O}_3$  grains. During particle ripening, small alumina particles dissolve into the glass and then precipitate on the large faceted  $\text{Al}_2\text{O}_3$  particles. In addition, the coalescence of neighboring particles could be an additional grain growth mechanism.

The growth of tabular grains is mainly along the basal plane of  $\alpha\text{-Al}_2\text{O}_3$ . The glassy phase contains about 5.0-mol%  $\text{Al}_2\text{O}_3$  content. The glass offers the route of heterogeneous nucleation of  $\text{Al}_2\text{O}_3$  grains preferentially taking place at the interface. Only the perpendicular growth of the  $\text{Al}_2\text{O}_3$  grains can reach the surface of the coating layer. A maximum grain growth rate of 3.6  $\mu\text{m}/\text{h}$  was measured at a temperature of 1450°C.

#### Acknowledgments

The authors would like to thank Professor S.-C. Wang for the help of one AEM analysis and Professor H. Schneider for his suggestions on the prevention of several unexpected sodium contaminations.

#### References

<sup>1</sup>W. D. Kingery, H. K. Bowen, and D. R. Uhlmann, *Introduction to Ceramics*, 2nd edition, John Wiley & Sons Inc., New York, 1976.

<sup>2</sup>M. Zhou, J. M. F. Ferreira, A. T. Fonseca, and J. L. Baptista, "In Situ Formed  $\alpha$ -Alumina Platelets in a Mullite-Alumina Composite," *J. Eur. Ceram. Soc.*, **18**, 495–500 (1998).

<sup>3</sup>Y. Ma and K. J. Bowman, "Texture in Hot Pressed or Forged Alumina," *J. Am. Ceram. Soc.*, **74** [11] 2941–4 (1991).

<sup>4</sup>M. M. Seabaugh, I. H. Kerscht, and G. L. Messing, "Texture Development by Templated Grain Growth in Liquid-Phase-Sintered  $\alpha$ -Alumina," *J. Am. Ceram. Soc.*, **80** [5] 1181–8 (1997).

<sup>5</sup>M. M. Seabaugh, M. D. Vaudin, J. P. Cline, and G. L. Messing, "Comparison of Texture Analysis Techniques for Highly Oriented  $\alpha\text{-Al}_2\text{O}_3$ ," *J. Am. Ceram. Soc.*, **83** [8] 2049–54 (2000).

<sup>6</sup>M. M. Seabaugh and G. L. Messing, "Texture Development and Microstructure Evolution in Liquid-Phase-Sintered  $\alpha$ -Alumina Ceramics Prepared by Templated Grain Growth," *J. Am. Ceram. Soc.*, **83** [12] 3109–16 (2000).

<sup>7</sup>A. Kebbede, G. L. Messing, and A. H. Carim, "Grain Boundaries in Titania-Doped  $\alpha$ -Alumina with Anisotropic Microstructure," *J. Am. Ceram. Soc.*, **80** [11] 2814–20 (1997).

<sup>8</sup>S. Kwon and G. L. Messing, "Sintering of Mixtures of Seeded Boehmite and Ultrafine  $\alpha$ -Alumina," *J. Am. Ceram. Soc.*, **83** [1] 82–8 (2000).

<sup>9</sup>W. C. Wei and J. W. Halloran, "Transformation Kinetics of Diphasic Aluminosilicate Gels," *J. Am. Ceram. Soc.*, **71** [7] 581–7 (1988).

<sup>10</sup>Y. Y. Chen, "Formation of Mullite Thin Film by Sol-Gel Process"; Master Thesis, NTU, 2001.

<sup>11</sup>W. C. J. Wei, S. J. Lu, and B.-K. Yu, "Characterization of Submicron Alumina Dispersions with Poly(Methylacrylic Acid) Polyelectrolyte," *J. Eur. Ceram. Soc.*, **15**, 154–64 (1995).

<sup>12</sup>Y. Y. Chen and W. C. J. Wei, "Formation of Mullite Thin Film Via a Sol-Gel Process with Polyvinylpyrrolidone Additive," *J. Eur. Ceram. Soc.*, **21**, 2535–40 (2001).

<sup>13</sup>B. Y. Yu, "Study on the Formation Mechanism of Tabular  $\text{Al}_2\text{O}_3$  and Prismatic Mullite Formation on Alumina Substrate"; Doctoral Dissertation, NTU, Taiwan, Republic of China, 2007.

<sup>14</sup>W. C. Wei and J. W. Halloran, "Phase Transformation of Diphasic Aluminosilicate Gels," *J. Am. Ceram. Soc.*, **71** [3] 166–72 (1988). □